

The Bulk RS KK-gluon at the LHC

Ben Lillie¹, Lisa Randall², Lian-Tao Wang³

¹ *Argonne National Lab, Argonne, IL. 60439*

& University of Chicago, Chicago, IL 60637

² *Department of Physics, Harvard University, Cambridge MA. 02138*

³ *Department of Physics, Princeton University, Princeton NJ. 08544*

Abstract

We study the possibility of discovering and measuring the properties of the lightest Kaluza-Klein excitation of the gluon in a Randall-Sundrum scenario where the Standard Model matter and gauge fields propagate in the bulk. The KK-gluon decays primarily into top quarks. We discuss how to use the $t\bar{t}$ final states to discover and probe the properties of the KK-gluon. Identification of highly energetic tops is crucial for this analysis. We show that conventional identification methods relying on well separated decay products will not work for heavy resonances but suggest alternative methods for top identification for energetic tops. We find, conservatively, that resonances with masses less than 5 TeV can be discovered if the algorithm to identify high p_T tops can reject the QCD background by a factor of 10. We also find that for similar or lighter masses the spin can be determined and for lighter masses the chirality of the coupling to $t\bar{t}$ can be measured. Since the energetic top pair final state is a generic signature for a large class of new physics as the top quark presumably couples most strongly to the electroweak symmetry breaking sector, the methods we have outlined to study the properties of the KK-gluon should also be important in other scenarios.

1 Introduction

Proposed higher-dimensional solutions to the hierarchy problem suggest novel experimental possibilities for the LHC. An interesting class of models falls in the so-called Randall-Sundrum scenario in with a single warped extra dimension [1]. In the original model the Standard Model (SM) fields were confined to a single brane. However models in which the SM fermions and gauge bosons propagate throughout all five dimensions [2, 3, 4] can have attractive features such as suppressing flavor-changing neutral currents, explaining the hierarchy of fermion masses [3], and allowing gauge coupling unification [5].

The first signal of such a framework should be the resonant production of the Kaluza-Klein (KK) excitations of the gauge bosons. Since the KK-gluons are the most strongly coupled of the new KK particles, they have the largest production rate and will likely be the first signal of this model. We study the potential reach for discovery of this state in this paper.

As we will see below, all gauge KK states decay primarily to $t\bar{t}$, so the KK modes of the electroweak bosons do not gain in signal significance by having cleaner decay channels. Although discovering the KK-gluon will not in itself definitively establish the underlying RS geometry, a generic composite model of electroweak symmetry breaking does not require the existence of a KK-gluon. Therefore observing such a state could be interpreted as evidence for an extra-dimensional scenario to be supplemented by further studies. Although it is certainly interesting, for example, to study decay modes such as $t^{(1)} \rightarrow g^{(1)} + t$, we focus here on the more generic decay mode $g^{(1)} \rightarrow t\bar{t}$.

The masses of KK fermions are generically comparable to the KK-gluons, so whether the decay of the gluon KK modes to fermion KK states is open or not is model-dependent. In order to account for the top quark mass, the top quark is likely to be localized towards the TeV brane or mostly composite as in the model of, for example, Ref. [4]. Since the KK-gluon is also localized towards the TeV brane, it has a large wavefunction overlap with other composite states so we expect the KK-gluon decays dominantly into $t\bar{t}$ final states. Since the mass of the KK-gluons should be $\mathcal{O}(\text{TeV})$, their decays give energetic top quark final states, which pose novel challenges to experimental searches.

In this paper we first study the discovery reach for a KK-gluon. We then study the determination of its spin assuming decay into highly energetic top quark final states. Efficient identification of the top quark final states will require the implementation of new experimental methods. The conventional method for top jet identification based on reconstruction from separate objects in the top decay (see, for example, [6, 7, 8]) won't work for much of the parameter range since the tops will be highly boosted. New approaches, such as identifying massive jets, merit careful investigation. In this paper we point out the importance of such a signal and consider the necessary degree of top-jet resolution. Detailed knowledge of the structure of jets as well as sophisticated detector simulation will be needed to determine the efficacy of this approach, which is beyond the scope of this paper. Therefore, rather than focusing on a specific strategy, we choose to parameterize these unknowns with a range of signal dilution factors to determine the discovery potential in each case. We assume this will be followed by further experimental study.

We will also consider the possible spin-determination efficiency as well as the question of the helicity of the top final state. This is particularly interesting because in the simplest implementation [4] of a composite top, the t_R is localized towards the TeV brane while (t_L, b_L) is almost flat, and therefore the top quarks from KK-gluon decays will be highly polarized.

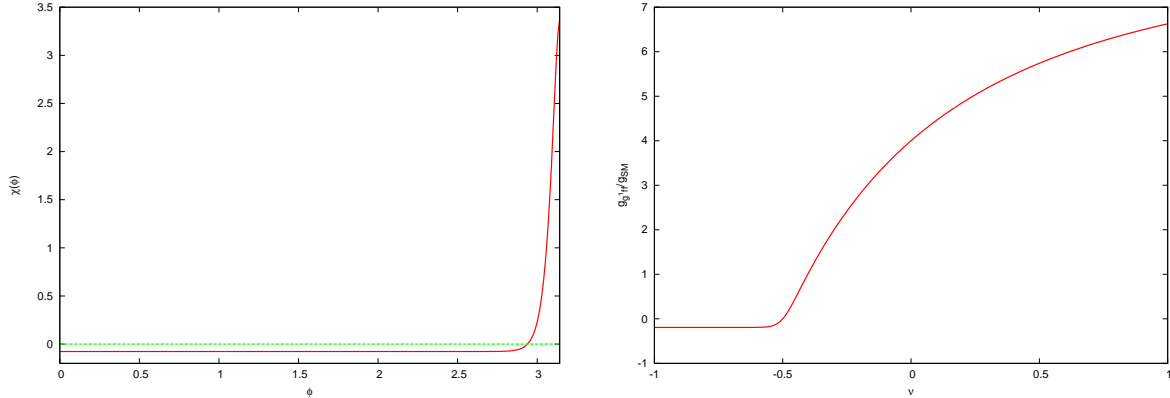


Figure 1: Left: Wavefunction of the first excited gauge KK mode. Note that it is extremely flat near the UV brane, with AdS_5 bulk coordinate defined by $y = \pi\phi$. Right: Coupling of the first gauge KK mode to a zero mode fermion as a function of the fermion localization parameter, ν . Notice that this coupling asymptotes quickly to a constant value for $\nu < -0.5$

2 Couplings between fermions and the KK gluon

The RS construction is a slice of 5 dimensional anti-deSitter space, AdS_5 , with metric

$$ds^2 = e^{-2\sigma} \eta_{\mu\nu} dx^\mu dx^\nu - dy^2 \quad (1)$$

where y is the coordinate of the 5th direction, and $\sigma = k|y|$ with k determining the curvature of the AdS_5 . The extra dimension has the geometry of the orbifold S_1/Z_2 . At either fixed point of the orbifold is a brane. One, at $y = 0$ is called the “Planck”, or “UV” brane; the other, at $y = \pm\pi r_c$, is the “TeV” or “IR” brane. If $kr_c \simeq 11$ then the warp factor at the IR brane, $\epsilon = e^{-\pi kr_c} = 10^{-15}$ is the ratio of the Planck to TeV scales¹.

The couplings between the SM fermions and the KK-gauge bosons, in particular the KK-gluon, determine most of the interesting phenomenological features of the model. We provide a brief summary of them here. See Appendix A for a detailed discussion of useful formalisms for describing gauge and fermion fields in AdS_5 .

We obtain the 4D effective couplings $g_{f\bar{f}A^{(n)}}$ by integrating over the 5th dimension. These couplings are sensitive to the profiles of the fermion and KK-gauge boson states in the bulk. Modulo certain brane kinetic terms, which we are not considering here, the profile of the KK-gluon is largely fixed, as can be seen in the left panel of Fig. 1. On the other hand, the wavefunctions of zero mode fermions are model dependent, and can be used to address the flavor hierarchy.

For a 5D fermion sector, we can write down a mass term $m_\Psi \bar{\Psi}\Psi$ for each 5d fermion field. Since Ψ is Dirac, we can write it as $\Psi = (\zeta \xi)^\top$ where ζ and ξ are Weyl spinors. We can write the mass as $m_\Psi = \nu_\Psi k \epsilon(y)$, where $\epsilon(y)$, which is 1 for $y > 0$ and -1 for $y < 0$, is responsible for making the mass term even under the orbifolding symmetry. The orbifold projection selects out one zero mode of one chirality. The wavefunction of the remaining zero mode is [3]

$$\xi_\Psi^{(0)} = \frac{e^{\nu_\Psi ky}}{N_f^{(0)}}, \quad (2)$$

¹For definiteness, we take $kr_c = 11.27$ to match to previous studies.

where $N_f^{(0)}$ is a normalization factor. This wavefunction is exponentially peaked toward the UV brane for $\nu < -1/2$ and toward the IR for $\nu > -1/2$.

Assuming $\mathcal{O}(1)$ 5D Yukawa couplings, the effective 4D Yukawa couplings are determined by the wavefunction overlap between the SM fermions and the TeV brane. Since the top quark Yukawa is very close to unity, the 3rd generation cannot be strongly UV localized. However, localizing the b_L (which, of course, comes in a doublet with the t_L) too close to the IR brane results in unacceptable deviations in the rate of $Z \rightarrow b\bar{b}$ [4]. This leads to the following set of parameters

$$\begin{aligned}\nu_{t_R} &\approx -0.3, \\ \nu_{Q_{3L}} &\approx -0.4, \\ \nu_{\text{other}} &< -0.5.\end{aligned}\tag{3}$$

That is: the t_R is IR localized, the third generation quark doublet, Q_{3L} is close to flat, and the others are all *UV* localized. This is important because the coupling of a zero mode fermion to a KK-gauge boson is dependent on the ν parameter. This coupling is given by² [2]

$$g_{f\bar{f}A^{(n)}} = g_4 \sqrt{2\pi k r_c} \left[\frac{1 + 2\nu}{1 - e^{2\nu+1}} \right] \int_\epsilon^1 dz z^{2\nu+1} \frac{J_1(x_n^A z) + \alpha_n^A Y_1(x_n^A)}{|J_1(x_n^A) + \alpha_n^A Y_1(x_n^A)|}.\tag{4}$$

The right panel of Fig. 1 shows the ratio of couplings, $g_{f\bar{f}A^{(1)}}/g_4$, for the first gauge KK mode. Note that for $\nu < -0.5$ the coupling is flat in ν and $g_{f\bar{f}g^{(1)}} \simeq 0.2g_4$, where the effective 4D gauge coupling of the $SU(3)_C$ gauge coupling in the Standard Model, $g_4 = g_s$. Notice that the production cross-section for the process $q\bar{q} \rightarrow g^{(1)}$ is not suppressed by M_P [9], as it is for the KK gravitons. This is generically true for any KK-resonances which are not singlets of the SM gauge symmetry. This fact can also be understood in the CFT dual as the effect of mixing between fundamental and composite states [10]. For the Q_{3L} doublet we have $g_{f\bar{f}g^{(1)}} \simeq g_s$, and for the t_R , $g_{f\bar{f}g^{(1)}} \simeq 4g_s$.

The fact that the coupling constant $g_{f\bar{f}A^{(n)}}$ approaches a constant results from near flatness of $A^{(n)}$ wave-function (as shown in Fig. 1) and the highly localized nature of the fermion wavefunction for $\nu < -0.5$ ($\propto \exp(-(1 + 2\nu)y)$ away from the Planck brane). Using the asymptotic form of the $A^{(n)}$ wave-function, we estimate from Eq. 4 [2]:

$$\frac{g_{f\bar{f}A^{(n)}}}{g_{\text{SM}}} \simeq -\frac{1}{\sqrt{\pi k r_c}} \frac{1}{\sqrt{n - 0.2}} + \mathcal{O}[(\pi k r_c)^{-3/2}].\tag{5}$$

The fact that this coupling is not exponentially suppressed [2] can be understood in the CFT picture as the result of kinetic mixing between the SM gauge field and the composite vector states (KK-gauge bosons in the AdS) [10].

Note that we are looking only at KK-gluon production from quarks. At tree-level the coupling of two zero-mode gluons to a KK mode is zero by orthogonality. Though there may be a loop-induced coupling, the main effect of this would be to increase the rate, since the gg channel will open. Neglecting it here is therefore a conservative assumption.

Constraints on the masses of the KK excitations of the electroweak gauge bosons from precision electroweak data give $M_{KK} \gtrsim 2 - 3$ TeV [4]. However, such a constraint is model-dependent. Since we are interested in generic properties of the KK-gluon, we present our result in a broader range of the KK-gluon mass.

²See the appendix for definitions of the symbols.

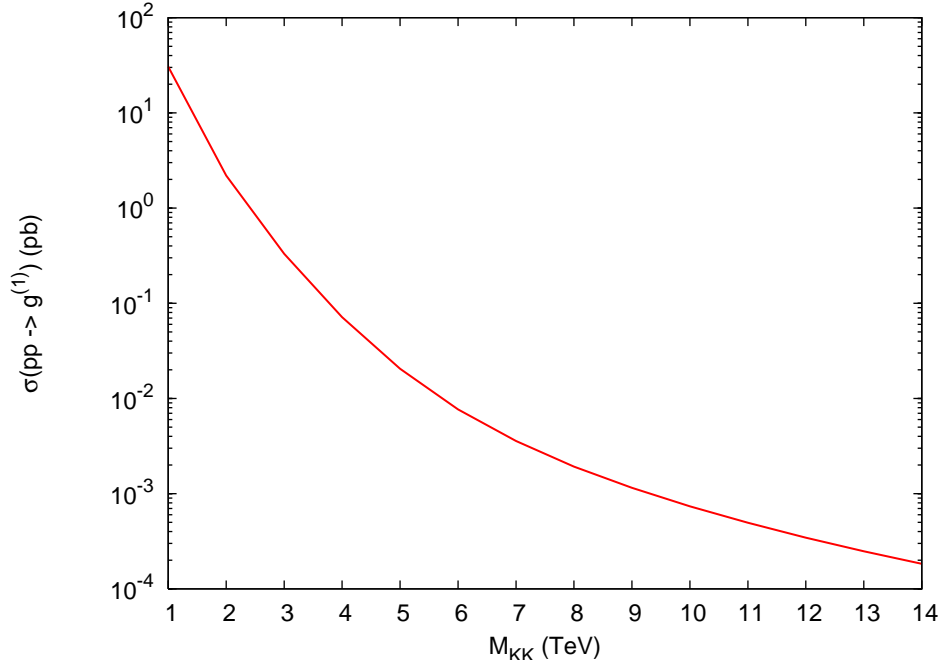


Figure 2: Total cross-section for production of the first KK gluon, as a function of KK mass.

3 Discovery

3.1 Cross Section

The KK excitations of the gluons will appear as resonances in the process $pp \rightarrow q\bar{q}$, primarily decaying in the $t\bar{t}$ channel. The branching ratio for $g^{(1)} \rightarrow t\bar{t}$ is 92.5% (and another 5.5% is to $b\bar{b}$, with the rest to light quark jets). To study the signal we have simulated the process $q\bar{q} \rightarrow g^{(1)} \rightarrow q\bar{q}$ using MADGRAPH and MADEVENT [12]. A plot of the inclusive cross section as a function of the resonance mass is shown in Fig. 2. The width of this resonance with the fermion configuration in Eq. 3 is

$$\Gamma/M \approx 0.17. \quad (6)$$

Figure 3 shows the $t\bar{t}$ invariant mass distribution from KK resonances, demonstrating that with efficient top quark identification it should be visible above the SM $t\bar{t}$ background up to relatively high masses. This will require reconstructing the $t\bar{t}$ pair to identify the relatively narrow resonance in the $m_{t\bar{t}}$ distribution. Clearly, identifying the top pairs will be crucial to the discovery and study of the KK-gluon and experiments will have to be as efficient as possible in identifying tops.

To emphasize the importance of top ID, consider the worst case scenario in which a top jet is not distinguished from a QCD jet. We compare the signal with QCD dijet production. We show the rates for dijets, with both pseudo-rapidities < 0.5 and the leading jet $p_T > 500$ GeV in Fig. 4. We see that even selecting the events to be very central and containing high p_T jets, signal identification is difficult. The raw dijet rate is overwhelming even with these cuts. Although more refined cuts could reduce the background, they are probably not enough without some top-quark ID.

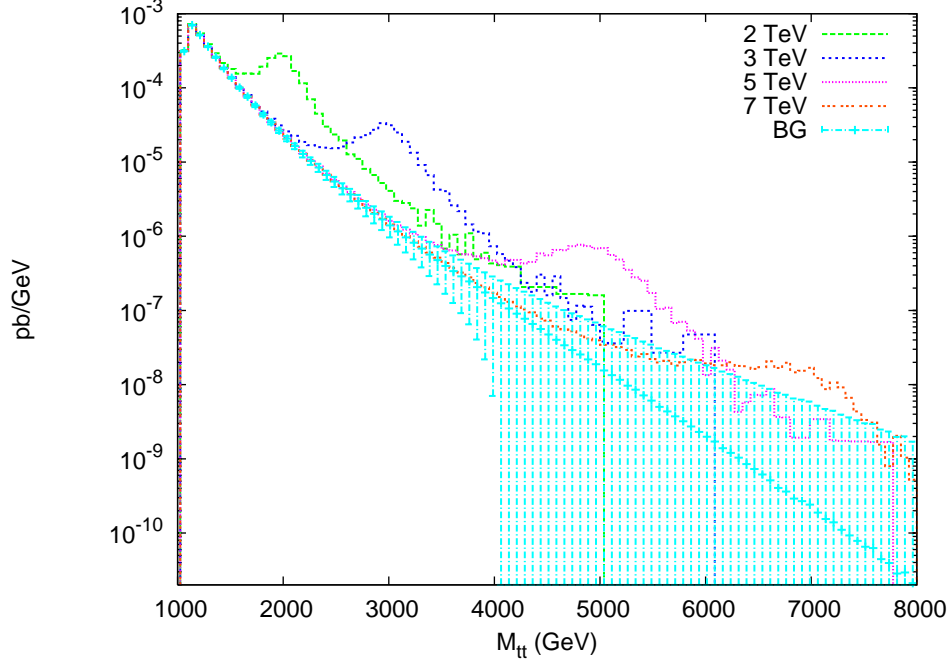


Figure 3: Invariant mass distribution of $t\bar{t}$ pairs coming from the KK gluon resonance, and SM $t\bar{t}$ production. The errors shown on the background curve are the statistical errors assuming 100 fb^{-1} of luminosity.

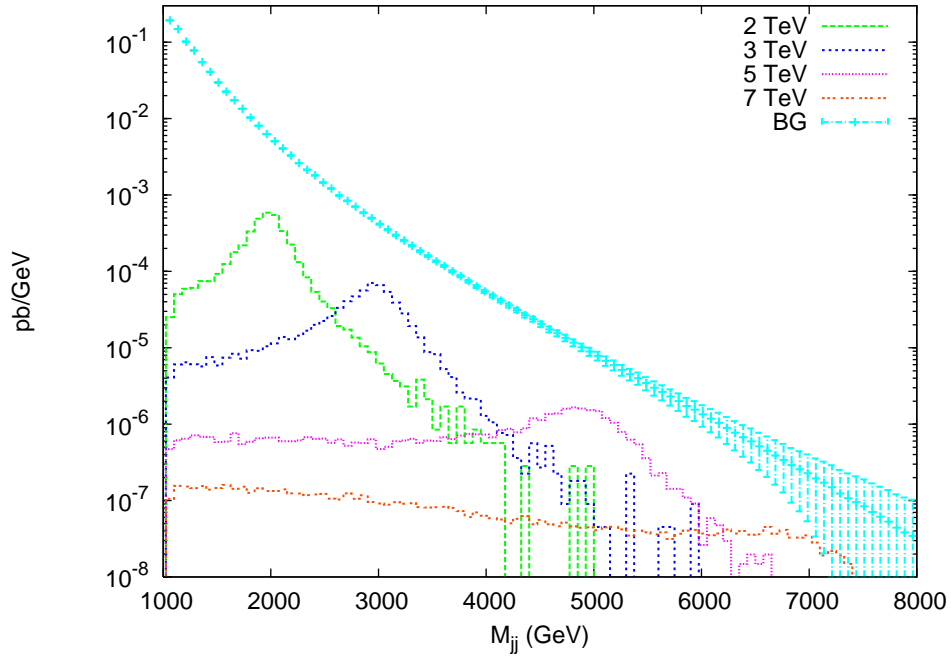


Figure 4: Invariant mass distribution of the decay products for several masses of the KK gluon. This assumes all $t\bar{t}$ events are fully collimated. “BG” is QCD dijet production. All jets are required to have pseudo-rapidities $|\eta| < 0.5$, and at least one to have $p_T > 500 \text{ GeV}$. The errors shown on the background curve are the statistical errors assuming 100 fb^{-1} of luminosity.

So before further further discussing the KK gluon resonance, we consider collider features of energetic top quarks decaying from the resonance in the next subsection.

We note that in principle $A^{(1)} \rightarrow W_L^+ W_L^-$ is also an important and generic decay modes for KK states, such as the KK states of the Z or gravitons, due to the large overlap between their wavefunctions and the longitudinal mode of W . However, such a decay mode does not exist for KK-gluon. In fact, we could treat such an absence as one other confirmation that the resonance is a KK-gluon.

3.2 Characteristics of energetic tops

In this section we discuss possible top quark collider signatures.

Top reconstruction in $t\bar{t}$ final states has been very well studied for relatively low invariant mass, $m_{t\bar{t}} \leq 1$ TeV. A crucial ingredient of the algorithm is detecting several separated objects from the decaying tops [6, 7, 8, 11]. For example, in the promising semi-leptonic decay, typically an isolated lepton and a b -jet on one side and three jets on the other side are required. However, we expect top quarks from $g^{(1)}$ decays to be very energetic, with $p_T \sim 0.5M_{g^{(1)}}$. Therefore, for such energetic top quarks (especially at the high end of the mass range) we expect the decay products will be highly collimated and the conventional reconstruction algorithm will fail.

To study this collimation, we have generated SM $t\bar{t}$ events in PYTHIA [13]. In Figs. 5 and 6, we discuss possible cuts relevant to top quark identification as a function of energy and top p_T . In these figures we have imposed a lower p_T cut and a window of invariant masses and then find the fraction of events which have a certain number of isolated objects (jets, leptons, or p_T). We use an isolation cut of $\Delta R = \sqrt{\Delta\eta^2 + \Delta\phi^2} > 0.4$, the smallest cone size generally considered for jets. We also show the fraction of events where at least one top is completely collimated, *i.e.* all three decay products are within 0.4 of each other.

For resonances heavier than 3 TeV, there is always a large portion, $> 90\%$, of the events with at least one top jet highly collimated. If these cannot be distinguished from QCD jets, the full QCD multi-jet cross-section would be the background for fully hadronic events, and the W +jets cross-section for the leptonic modes. This is in addition to other reducible backgrounds. Carefully chosen cuts may reduce these. Nonetheless, it is clear that an effective strategy for identifying highly collimated tops and distinguishing them from QCD jets will be essential to identifying $t\bar{t}$ events in this kinematical regime.

We also see that for $M_{KK} > 3(4)$ TeV, a significant portion 30%(70%) of events will have only two well isolated objects. Clearly here the problem of identifying highly collimated top quarks is the most serious and the most critical. In order to not be swamped by the QCD dijet background, new ways of identifying these highly collimated top jets will be essential. For $M_{KK} < 2$ TeV, we expect the conventional method of reconstructing two tops from six distinct objects will work, at least for the majority of the events.

Notice that top collimation, within a particular window of $m_{t\bar{t}}$, the collimation depends strongly on p_T . This stems from the difference in boosting a central and a forward top. For a forward top, it is generically easier for the decay product to have a large ϕ separation. At the same time, the boost also has less effect on $\Delta\eta$, since it is an invariant if the top is moving along the z -direction. Therefore, forward top quarks tend to have more separated decay products. At the same time, within an invariant mass window, a p_T cut tends to force the tops to be more central. This seems to indicate that we should focus on more forward tops. However, notice that SM $t\bar{t}$ background is even more forward, and a strong p_T cut is usually necessary to suppress those backgrounds. Therefore, we have to deal with the more severe collimation

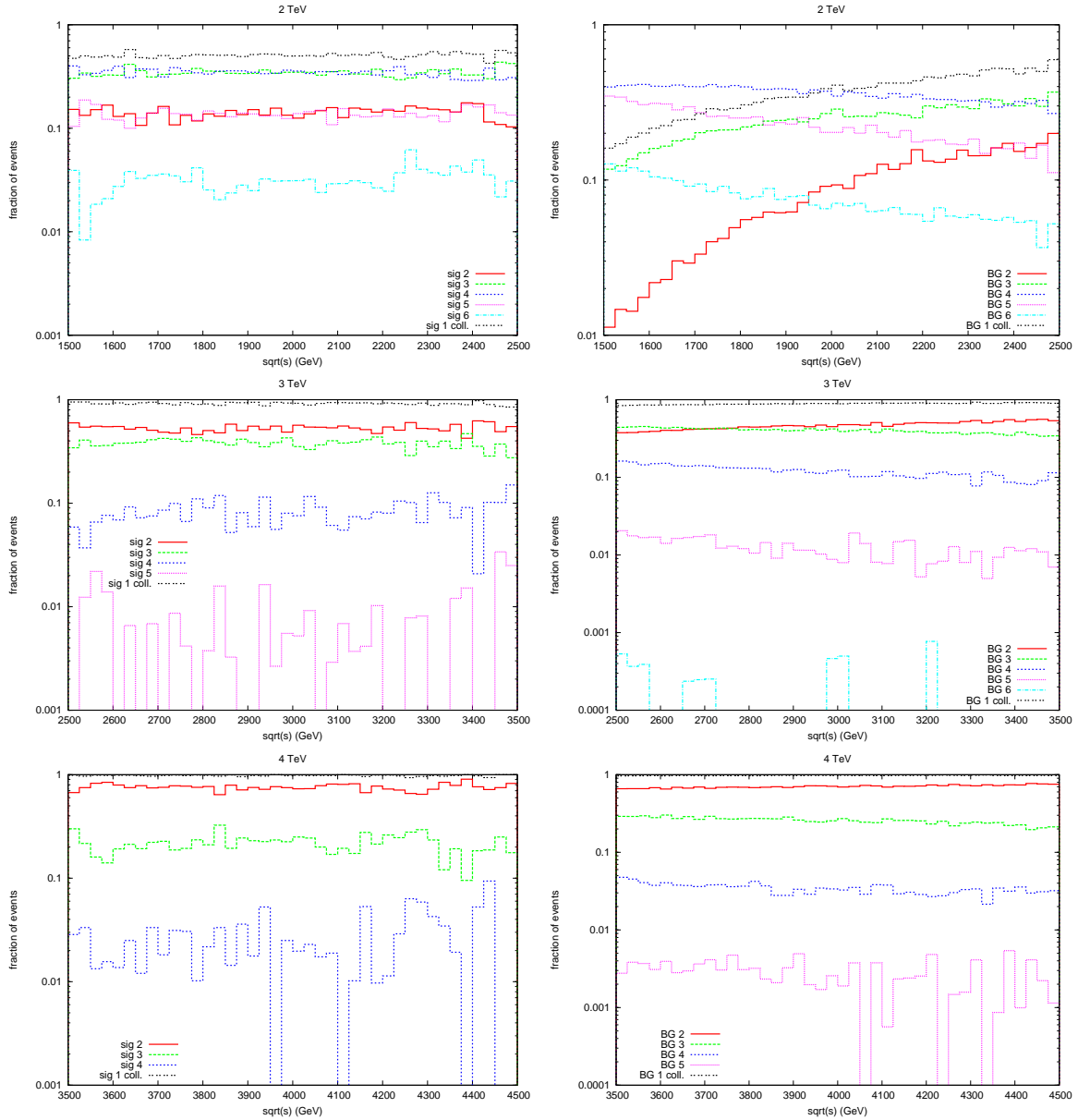


Figure 5: Left: Fraction of events with certain numbers of distinct objects for events from decay of a KK gluon, with mass (top to bottom) 2, 3, and 4 TeV as a function of invariant mass of the $t\bar{t}$ pair, after imposing a cut on the top p_T : 500 GeV, 1 TeV, and 1.5 TeV. Right: SM $t\bar{t}$ production using the same cuts as the corresponding plot on the right. The line labeled “1 coll.” is the fraction of events where at least one of the tops has all three decay products within the same cone. A cone size of 0.4 has been used.

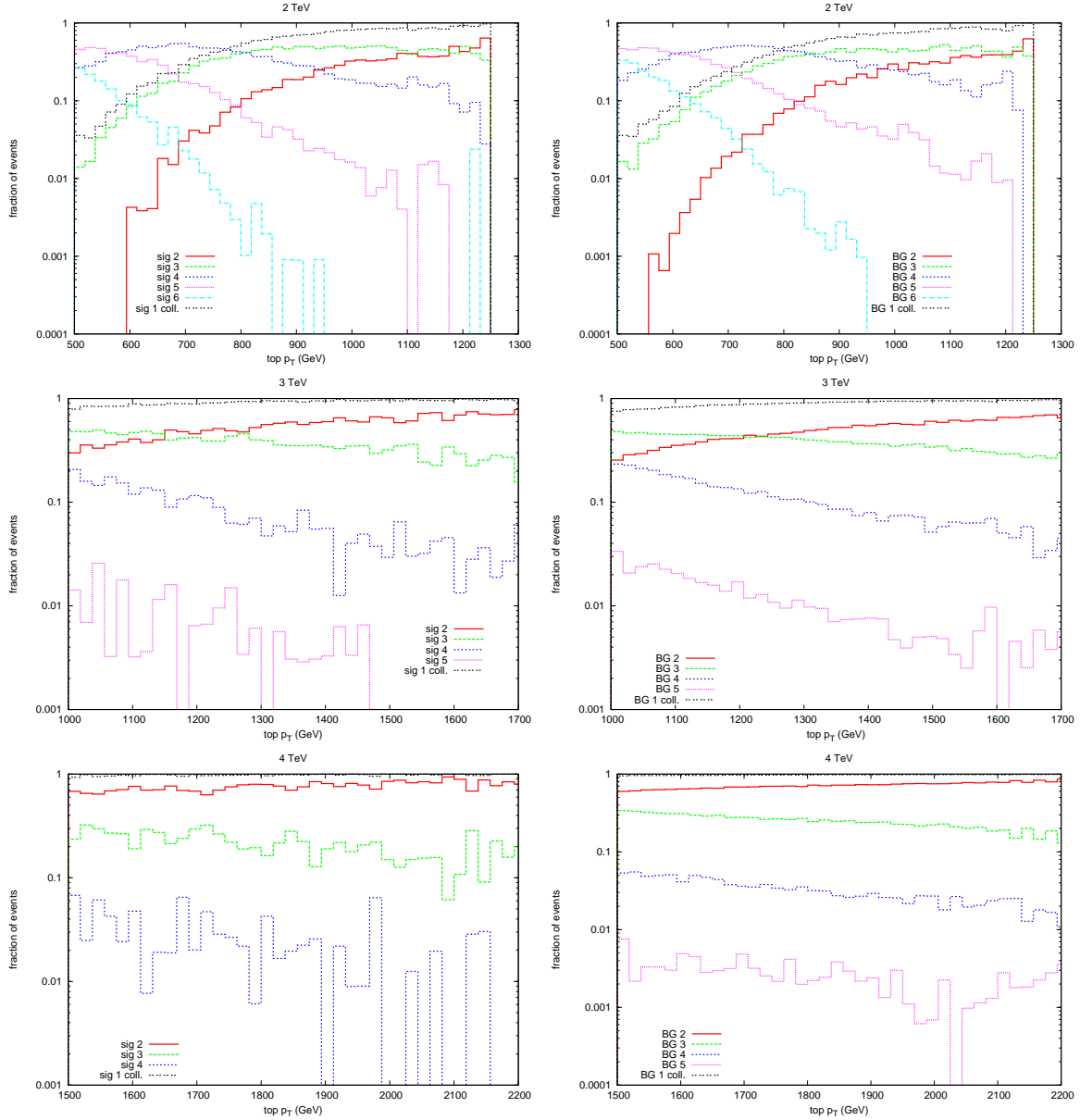


Figure 6: Left: Fraction of events for certain numbers of distinct objects for events from decay of a KK gluon, with mass (top to bottom) 2, 3, and 4 TeV as a function of p_T for events in the window $m_{KK} - 500 \text{ GeV} < m_{t\bar{t}} < m_{KK} + 500 \text{ GeV}$. Right: SM $t\bar{t}$ production using the same cuts as the corresponding plot on the right. The line labeled “1 coll.” is the fraction of events where at least one of the tops has all three decay products within the same cone. A cone size of 0.4 has been used.

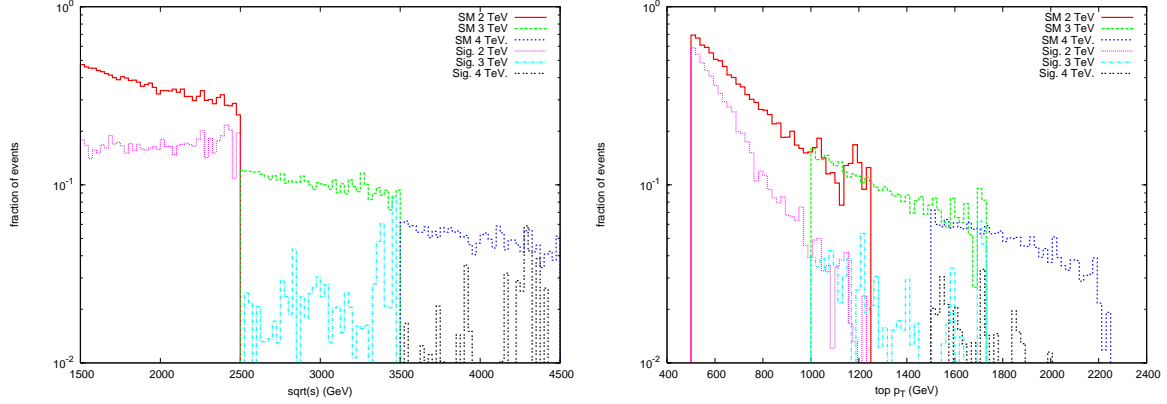


Figure 7: Left: Fraction of events where at least 1 top decays leptonically with an isolated lepton. The cuts imposed are: $\text{top } p_T > (500, 1,000, 1,500)$ GeV for KK masses (2,3,4) TeV, the invariant mass in a window 1 TeV wide around the resonance. The lines labeled "SM" are for SM $t\bar{t}$ production with the same cuts.

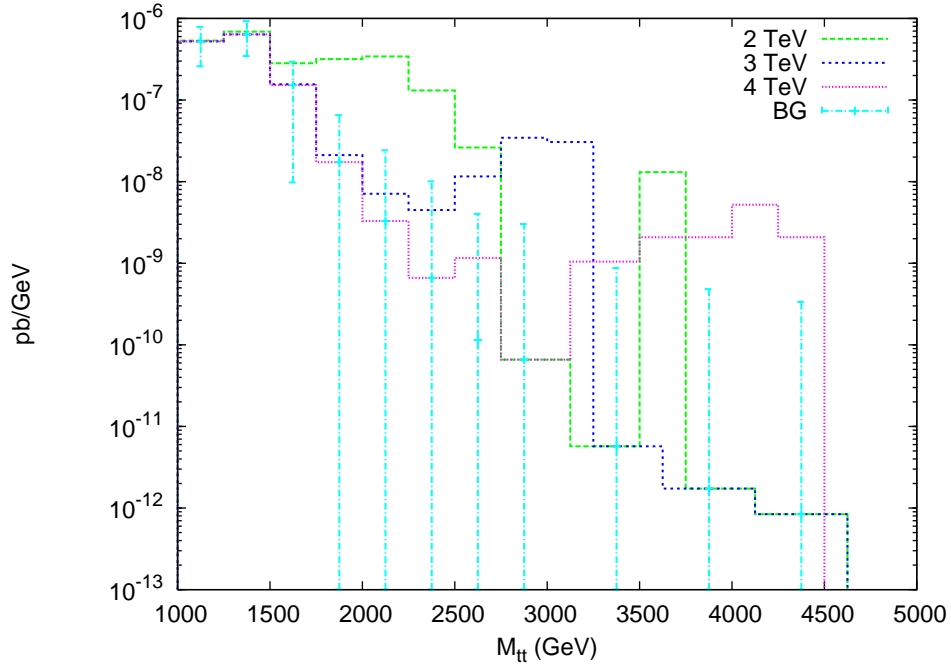


Figure 8: Invariant mass distribution for events where at least 1 lepton is isolated. A p_T cut of 500 GeV on one of the tops has been used.

problem for the central tops.

Lepton isolation is also important for a variety of reasons. It points toward a class of cleaner events. It is also important in measurements such as top helicity, as we discuss in Section 4. In Fig. 7 we plot the fraction of events with an isolated lepton, with the same cuts as used above. We see that, if $M_{KK} > 3$ TeV, only a few % of the signal events have an isolated lepton. Note also the difference between signal and background, which is due to the fact that the signal events are more central than the background events. Of course, even with an isolated lepton, we still have to deal with the fact that the other side of the same event will have the collimation problem alluded to above. Since the fraction of events with an isolated lepton is different between the signal and background, we can not estimate the relative rates simply by scaling Fig. 3. To understand the relative rates between signal and background, in Fig. 8 we show the invariant mass distribution of events with a separated lepton. We see that, with a p_T cut of 500 GeV on one of the tops the signal does indeed dominate over the background, but that the event rate is becoming low.

Over the mass range $2 \text{ TeV} < M_{KK} < 3 \text{ TeV}$, there are a wide variety of event configurations featuring from 2 to 5 separated objects with different portions depending on mass and all these cases need to be considered. Each of them will be a combination of partial reconstruction and/or identification of collimated top jets. Each of them, depending on which object is isolated, will have to include different backgrounds. A complete study, certainly important and interesting, is beyond the scope of this paper. When there are more than two jets, we expect the reconstruction efficiency to be somewhat better than the two objects case due to the additional handle of the extra separated objects, but a quantitative assessment is required.

We now comment on possible techniques for identifying the highly collimated "top-jets". If jets can be identified as originating from top quarks, even without explicitly separated decay products, one can nonetheless identify the resonance structure in the $t\bar{t}$ invariant mass distribution as well as the angular distributions of the tops, which carries the spin information of the initial KK-gluon state.

One route is to always demand some partial separation between some of the objects, such as a b and a lepton. Indeed, this is probably what one has to do in order to measure the top quark helicity, and we have seen that this will likely work very well for KK masses < 2 TeV, and will probably work for masses $\lesssim 3$ TeV. It is probably somewhat easier to do independent lepton identification for muons than for electrons, depending on ECAL performance, and the understanding of the EM energy content of high p_T jets. At the same time, the question still remains how to reconstruct or identify the other side (hadronic) as a potential top candidate. Moreover, even demanding only a single isolated lepton without any cuts on the other decay products, we see that the event rate takes a big hit when $M_{g^{(1)}} \gtrsim 2$ TeV.

Most efficient top tagging algorithms will require the existence of a b -tag. However, tagging an energetic b -quark with additional objects close to it will be challenging so the tagging rate at high p_T is still uncertain. In particular one should worry that the high boost of the b will cause the opening angle of the b decay products to close beyond the resolution of the detector. It is also possible that the merging of the b -jet with the other top decay products will cause the b -tagging efficiency for the signal to be lower than that for the background.

Other strategies for identifying top quarks will exploit the differences between a top jet and a normal jet. One distinguishing feature of the top jet is its large invariant mass. Some massive jet algorithms, for example, similar to those used in identifying hadronic W s in WW scattering [14], might be useful for identifying a top jet. However, QCD processes could produce massive jets with off-shell partons and hard radiations. For example, the average jet mass,

conventionally defined, for jets with high p_T peaks at around 15% of the jet p_T [15] so a full background study is required.

One additional important aspect of top-jets might be sub-structure, which can potentially be probed by using more detailed features of events. For example, sub-clusters at the tracking level could be particularly useful since the inner detectors usually have finer granularity than calorimeters. Variables one might want to study include sub-cluster with a common impact parameter, or more than two subclusters. The presence of high p_T leptons merged with the jets may also prove useful. A jet where a large fraction of the energy is contained in one muon, for example, is unusual for QCD jets.

With the extreme importance of the top signal in mind, it is worthwhile to study these questions in much greater detail. Any such strategy will have to be optimized, probably for every particular mass region, to gain maximal efficiency and reduce fake rate. Different strategies will involve different backgrounds which could fake the signal. As such a study is beyond the scope of this paper, we will demonstrate the main features of KK-gluon phenomenology by parameterizing the degrading of the signal with a range of fake rates and leave detailed studies of the suggested methods to the future.

3.3 Extracting the KK-gluon signal

In this section, we study how well the signal can be extracted over background. We present the signal in Fig. 4. Note an interesting feature of the high mass resonance signal. The events are almost pure s -channel resonant production yet most of the events from the high-mass resonances show up at low invariant mass, many widths away from the resonance. This is due to the steeply falling PDFs in the region of the resonance which compensates the suppression from high virtuality.

We first consider the extent to which b -tagging could help. If we assume 50% efficiency and a 1% fake rate [7], both for the signal and the background and demand one b -tag we get the distributions shown in Fig. 9. These numbers for b -tagging performance are almost certain to be wrong at high p_T , but this provides an optimistic estimate in the absence of a detailed study in the range of p_T considered here. We see that there is some possibility that the resonance will be observable just by requiring a single b -tag if it is highly efficient, as assumed here.

Notice that we can also conclude from this plot that the b_L final states are unlikely to be useful for discovering the resonance. The rate is reduced by a factor of 17 relative to top quark production. Since the background in Figure 9 that remains after b -tagging is predominantly $b\bar{b}$, we can see that the signal will be swamped by the background.

In general, to identify the energetic top quarks, new techniques will be required. Developing a proper top-tagging algorithm is beyond the scope of this paper. As stated in the previous subsection, we will instead investigate the behavior of the signal with different assumptions for the performance of such an algorithm.

Every top identification strategy will introduce fakes from its own background. The strategy we consider with two object final states will inevitably have to contend with, among other backgrounds, fakes from the QCD dijet and $b\bar{b}$ backgrounds. Given the size of the dijet and $b\bar{b}$ rates, the important feature of top identification will be more background rejection than signal efficiency. We have simulated this by assuming a rate for dijet events faking $t\bar{t}$ events. The resulting invariant mass distributions for resonances of 2 and 5 TeV are plotted in Fig. 10.

From the plot, we conclude that extraction of the signal will require a background rejection of about a factor of 10. Notice that since we do not include a reduction factor on the $t\bar{t}$ (both

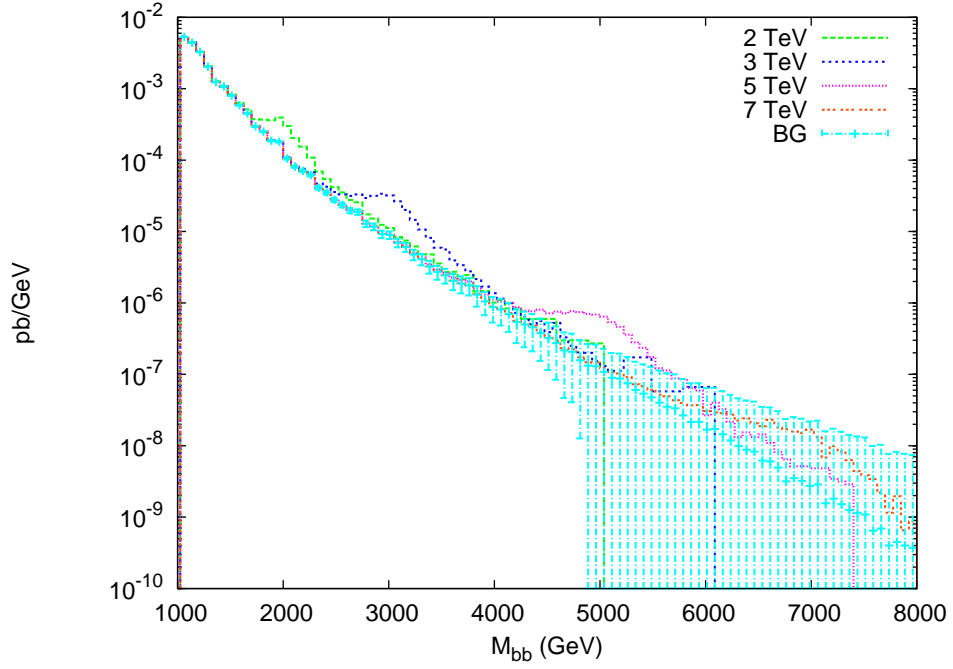


Figure 9: Same as in the previous figure, but requiring 1 b -tag. All signal curves have also been added to the background curve.

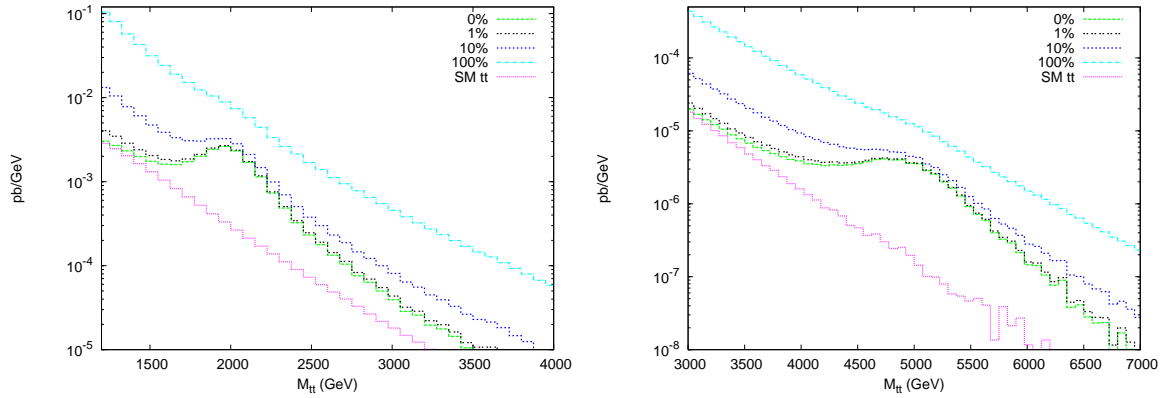


Figure 10: $t\bar{t}$ invariant mass distribution for signal plus some background assuming various values of the t -tagging fake rate for a resonance at 2 (left) and 5 (right) TeV.

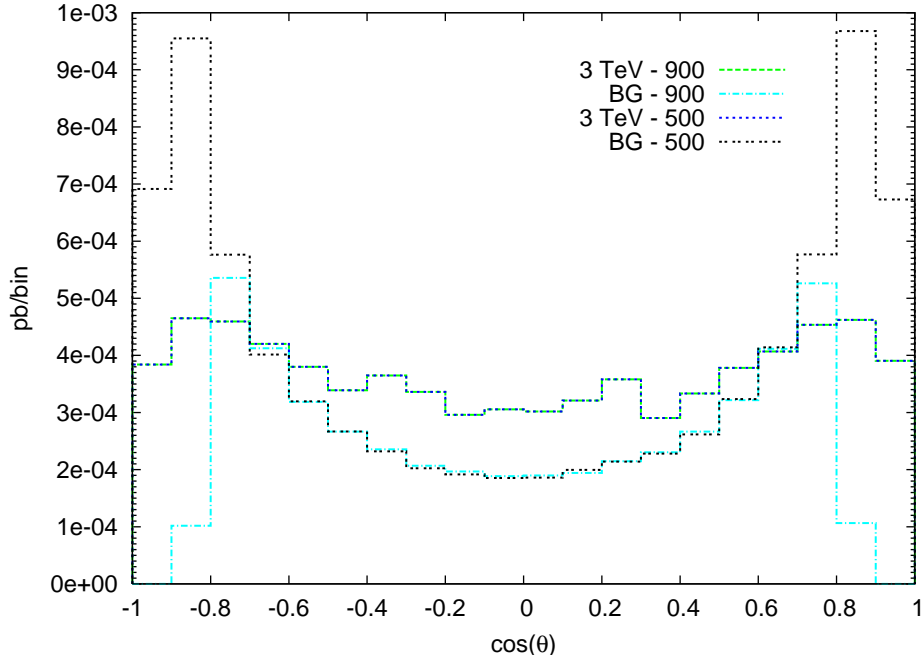


Figure 11: Distribution of $\cos\theta$, the decay angle in the hard-scattering CM frame, from a 3 TeV KK-gluon resonance. We show signal and background for two different choices of p_T cuts.

signal and background), the result presented here will be similar to a more inclusive algorithm which is optimized to include as much $t\bar{t}$ as possible. More refined balance may have to be sought between purity and efficiency in a completely realistic study.

For a 5 TeV resonance, a rejection factor of 10 for the dijet events produces a signal to background ratio of $S/B \sim 1$. Comparing Figs. 3 and 8 we can see that this is true for all KK masses we have considered. So a rejection factor of 10 will allow discovery as long as the luminosity is high enough to produce sufficiently many events. For 100 fb^{-1} , a resonance at 6 TeV will produce about 10 events after signal cuts. While it may be possible to discover a resonance with so few events, it would take a careful detector-level study to determine if this is indeed possible. Hence, our conservative estimate is that resonances with masses up to 5 TeV could be discovered at the LHC. The luminosity upgraded SLHC will likely extend this reach.

3.4 Spin measurement

After finding a resonance, it will be important to determine its properties. One important question is the spin of the resonance. Since the KK-gluons are produced via the process $q\bar{q} \rightarrow g^{(1)}$, we expect its decay products will reproduce the familiar $1 + \cos^2\theta$ distribution in the rest frame of the KK-gluon.

Finding the spin, i.e., probing the $(1 + \cos^2\theta)$ structure of the distribution, requires making use of the full angular acceptance of the central detector. Here, we used a 3 TeV KK-gluon as an example, though the results are similar for other masses. We require that the top decay products are all restricted to the range $|\eta| < 2.5$, and that the invariant mass is in a narrow window around the resonance, $2800 < m_{t\bar{t}} < 3500$. Since the background is steeply falling, we use a window that is asymmetric around $m_{t\bar{t}}$, with the lower bound being closer to $m_{t\bar{t}}$ than the upper bound. This should enhance the signal to background ratio. Additionally, because the

masses are large we can further enhance this ratio by imposing a strong p_T cut on either the reconstructed top or the top-jet. We plot the angular distributions in Fig 11 for two different cuts on p_T , either 500 or 900 GeV. We see that a suitably strong p_T cut has very small effect on the signal. This is expected since the p_T s of the tops are peaked around $0.5 M_{KK}$. On the other hand, such a cut is quite effective in suppressing the background. Crucial information about a $(1 + \cos^2 \theta)$ distribution comes from the more forward part of the distribution. However, the background is also strongly peaked forward. We see that an appropriate p_T cut could effectively reduce this part of the background.

4 Partial compositeness of t_R

As has been known for more than a decade, spin-correlation [16] in $t\bar{t}$ production provides an important probe of the structure of the Standard Model. It has since become an important subject for experimental study [17], and will be explored in much more detail at the LHC [18].

With the $t\bar{t}$ final states produced from the decay of some heavy new physics resonances well beyond twice the top mass, spin polarization measurements of the tops produced in the decay should be another powerful tool for probing new states, such the KK-gluon, which is likely to be mostly coupled to right-handed tops. In this section we will demonstrate the significance of the spin polarization measurement³.

Top quarks produced from a particular vertex will be of some definite chirality depending on the vertex. Such a state will generically be a mixture of helicity eigenstates since chiral symmetry is broken by the top quark mass. However, if very energetic top quarks are produced, they will be approximately in a helicity eigenstate, (to the order of $\mathcal{O}(m_t/E)$). Therefore, such top quarks could be thought of as a good chirality analyzers since their helicities carry the information of initial chirality of the coupling.

Extraction of the helicity of the top quark follows from a well-known procedure [16, 17, 18]. We consider here the leptonic decay mode $t \rightarrow bW^+ \rightarrow b\ell^+\nu$. In the rest frame of the top quark, the direction of top three-momentum $\hat{\mathbf{k}}$ defines the axis of polarization, i.e., the helicity of the top quark. We first consider the case in which the top is right-handed. Due to the $V - A$ nature of the Standard Model weak interaction, bottom quarks from top decay must be left handed. Depending on whether the b_L goes along or opposite to the direction of the top, angular momentum conservation requires that the W will be polarized either along $\hat{\mathbf{k}}$ ($|J = 1, m = 1 \rangle$)⁴ or longitudinally ($|J = 1, m = 0 \rangle$), respectively. Angular momentum conservation and $V - A$ again require ℓ^+ will always be correlated state of W polarization, either goes along the direction of its polarization for $|J = 1, m = 1 \rangle$ state, or goes perpendicular to the polarization axis for $|J = 1, m = 0 \rangle$ state. Combining these arguments, we conclude that ℓ^+ will always prefer to go along (or perpendicular) to $\hat{\mathbf{k}}$, but not opposite to it⁵.

In the case of a left-handed polarized top quark, a similar argument leads to the conclusion that ℓ^+ will prefer to go along the opposite (or perpendicular) to $\hat{\mathbf{k}}$. A careful treatment shows

³Other measurements of the chirality of the coupling come from forward backward asymmetry measurements and left-right asymmetries. These measurements give important Z-pole observables. However, the forward-backward asymmetry measurement requires both the product vertex and the decay vertex of the resonance to be chiral, which is not generically satisfied [4] for the KK-gluon since both the left and right handed quarks of the first two generations are localized towards the Planck brane. Clearly a left-right asymmetry measurement is impossible at a hadron collider.

⁴We have used $\hat{\mathbf{k}}$ to define the polarization axis for W .

⁵A very nice discussion of this can be found in [19].

that

$$\frac{d\Gamma}{\Gamma d\cos\phi_i} = \frac{1}{2}(1 + \alpha_i \cos\phi_i) \quad (7)$$

where i labels the decay product, and α_i is a constant. For the lepton (or down-type jet) $\alpha_\ell = 1$ at leading order, while for the b and neutrino (or up-type jet) $\alpha_i \approx -0.44$; NLO corrections to the α_i are known to be of order 1% [18].

Therefore, by measuring the angular distribution of the ℓ^+ in the rest frame of the t with respect to $\hat{\mathbf{k}}$, we will be able to establish the initial polarization of the top produced. Therefore, in the process of $g^{(1)} \rightarrow t\bar{t}$, due to the correlation between helicity and initial chirality, measurement of such angular correlation will establish the chirality of the $g^{(1)} - t - \bar{t}$ coupling.

We demonstrate such a measurement in the simple setup of [4], where we expect this coupling is dominantly right-handed. For this we use the full matrix element for $pp \rightarrow t\bar{t} \rightarrow e^+\nu_e b\bar{b}jj$, generated from MADGRAPH. Figure 12 shows the angular distribution for a 3 TeV resonance (without background) and for QCD top production. With an isolated lepton it should be simple to extract the top polarization. This tells us that such a measurement will be possible for KK masses up to ~ 2 to 3 TeV where the lepton isolation is difficult.

Another possibility is to use the p_T spectrum of the lepton as a proxy for the top polarization, as was done in studies of the W helicity in top decays at the Tevatron [20]. To illustrate this we looked at a 2 TeV resonance with 3 different sets of couplings. One is coupled in the same way as the rest of this paper; one where the left and right handed couplings to tops are switched; and finally one where the coupling is vector like. In all cases the sizes of the couplings were chosen to keep the width constant. We plotted the normalized lepton p_T spectra in Fig 13. This technique could, in principle, be used to study higher mass resonances since it does not depend on the lepton being isolated.

5 Conclusions

In this paper, we have studied the $t\bar{t}$ final state as a discovery mode and probe of the KK-gluon properties in the RS scenario where Standard Model fields are propagating in the bulk. We pointed out that for the energetic tops decaying from resonances with mass ≥ 2 TeV, conventional top reconstruction methods will be limited, despite the high production rate. Without some top jet identification, the signal will be swamped simply by the QCD dijet background.

We showed that b -tagging information will help reduce the background. However in order to efficiently identify the energetic tops, more detailed information from the top jets will be required. Implementation of such a strategy will certainly require detailed knowledge of the top “jet” structure and detector response to it. Given the importance of such a signal, it merits more detailed study. At the same time, any such method could not completely eliminate the fakes from background, such as QCD dijets and $b\bar{b}$ pairs. In the current study, we studied the question of how much discrimination power against such fakes is required in order to have a significant signal and take advantage of the big cross section for KK-gluon production and subsequent decay to the $t\bar{t}$ final state. In a study in which we parameterize the fake rate, we found that a rejection power of a factor of 10 is required in order to achieve this goal.

We also considered the angular correlations of the decay products of the top quarks to deduce the top quark helicity. Decaying from some heavy resonance, the top quarks are very

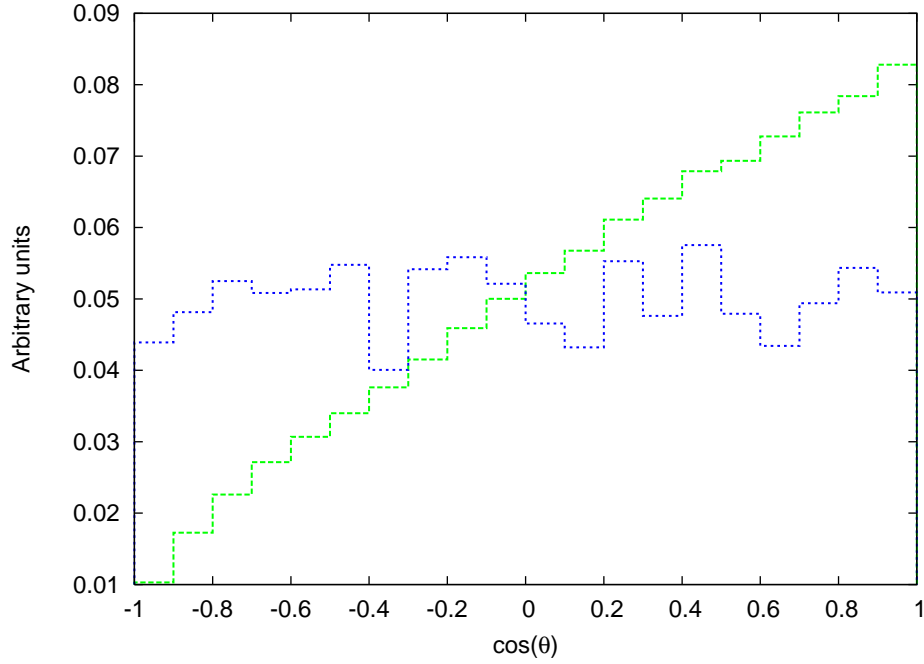


Figure 12: Normalized distribution $\cos(\phi)$, defined in the text, for a 3 TeV resonance (blue, dotted), and for QCD top production (green, dashed).

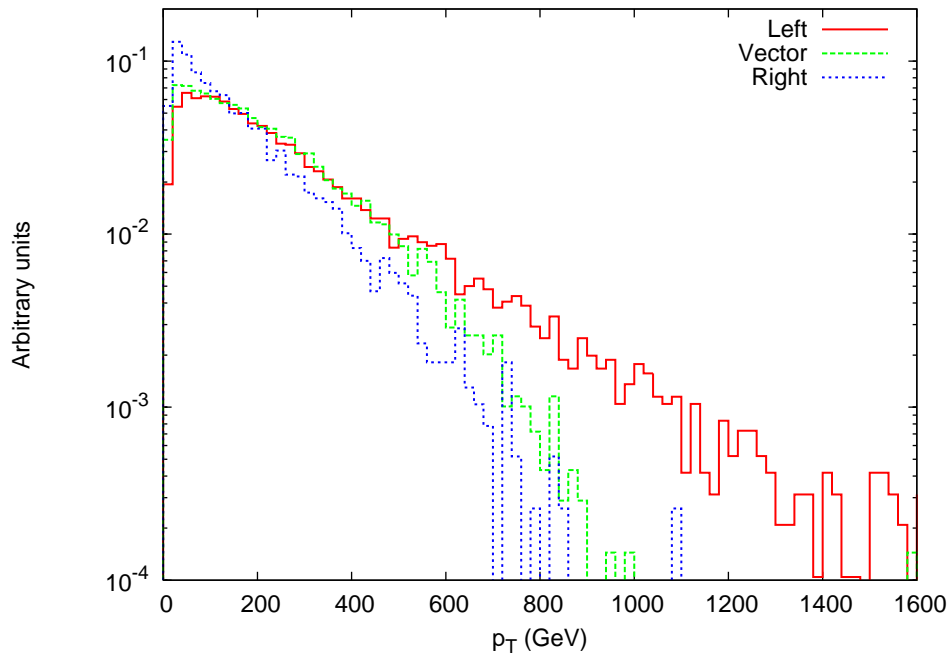


Figure 13: Distribution of lepton p_T from the process $pp \rightarrow t\bar{t} \rightarrow e^+\nu_e b\bar{b}jj$ for three resonances. One coupled like the KK gluon described in the text (“Right”), one where the couplings to left and right handed tops have been reversed (“Left”) and one coupled equally to left and right (“Vector”).

boosted. Therefore, the helicity is highly correlated with the chiral structure of the decay vertex. Such a measurement is crucial to probe the profiles of the SM fermions in the bulk. In the simple setup [4], the KK-gluon couples dominantly to right-handed top quarks. We demonstrated ways to establish the right-handed nature of such coupling, through conventional correlation observable in the top rest frame, as well as a p_T^ℓ observable.

Additionally, we remark that top quarks are most likely to be strongly coupled to any model of the electroweak sector and therefore identifying top quark jets could be one of the more important experimental goals. In particular the top jet final state should be an important signature for any strongly interacting new physics for which top quarks are somewhat special, such as composite models or topcolor models. Although we have focused on KK-gluons and using [4] as an example, we expect many lessons we have started to learn here will have a wide range of applicability.

Finally, we comment on, Ref. [21] which appeared recently and has overlap with our study. We note that there are several differences in the approach, scope, and results. Most noticeably, they have focused on a particular method of identify hadronic tops without taking advantage of the top jet properties. Hence, strong cuts are imposed, which could underestimate the discovery potential. They used helicity of the t_R as a way sharpening the signal. While it is certainly a useful approach, we remark that such a property is model dependent. In principle, it should come as a result of the measurement.

6 Acknowledgments

We would like to thank T. Han, Joey Huston, Greg Landsburg, Tom LeCompte, Liam Fitzpatrick, Jared Kaplan, Zack Sullivan, Tim Tait, and Chris Tully for useful discussions. B.L. is supported by the Department of Energy contract DE-AC02-06CH11357. The work of L.W. is supported by the National Science Foundation under Grant No. 0243680 and the Department of Energy under grant DE-FG02-90ER40542. Any opinions, findings, and conclusions or recommendations expressed in this material are those of the author(s) and do not necessarily reflect the views of the National Science Foundation.

A Formalisms

We are particularly interested in a model where all Standard Model (SM) fields except the Higgs propagate in the entire 5-d spacetime, and will be primarily concerned with the gluon and colored fermion fields. The pure gauge action for the gluons is the standard⁶

$$S_{\text{gluon}} = \int d^5x \sqrt{g} - \frac{1}{4} F_{\mu\nu}^a F^{\mu\nu a}. \quad (8)$$

We employ the gauge $A_5 = 0$, do a standard KK reduction

$$A_\mu^a(x, y) = \sum_n A_\mu^{a(n)} \frac{\chi^{(n)}(y)}{\sqrt{r_c}}, \quad (9)$$

⁶The indices M, N run over $(0, 1, 2, 3, 5)$, while μ, ν run over $(01, 2, 3)$; a is a gauge index.

and solve for the wavefunctions $\chi^{(n)}$. The solution for the wavefunction of the n -th KK mode is[2]

$$\chi_A^{(n)} = \frac{e^{k\pi\phi}}{N_A^{(n)}} \left[J_1(m_A^{(n)} e^{k\pi\phi}/k) + \alpha_A^{(n)} Y_1(m_A^{(n)} e^{k\pi\phi}/k) \right]. \quad (10)$$

Here J_1 and Y_1 are the standard Bessel functions of the first and second kind, $m_A^{(n)}$ is the mass of the n th KK mode, and $N_A^{(n)}$ is a normalization factor. Note that for an unbroken gauge group there is a zero mode which is flat in the extra dimension, $\chi^{(0)} = 1/\sqrt{2\pi}$.

For the fermion sector, note that in five dimensions there is no chirality. We can thus always write down a mass term for each 5d fermion field. Hence the fermion action for a single species, Ψ , is

$$S_{\text{fermion}} \int d^5x \bar{\Psi} i \not{D} \Psi + m_\Psi \bar{\Psi} \Psi. \quad (11)$$

Since Ψ is Dirac, we can write it as $\Psi = (\zeta \ \xi)^\top$ where ζ and ξ are Majorana spinors. We can write the mass as $m_\Psi = \nu_\Psi k \epsilon(y)$, where $\epsilon(y)$, which is 1 for $y > 0$ and -1 for $y < 0$, is responsible for making the mass term even under the orbifolding symmetry. The orbifolding projects out the zero mode of one chirality. The wavefunction of the remaining zero mode is[3]

$$\xi_\Psi^{(0)} = \frac{e^{\nu_\Psi k \pi \phi}}{N_f^{(0)}}, \quad (12)$$

where again $N_f^{(0)}$ is a normalization factor. This wavefunction is exponentially peaked toward the UV brane for $\nu < -1/2$ and toward the IR for $\nu > -1/2$. These zero modes correspond to the observed SM fermions, and will acquire masses from the Higgs vev in the normal way. Since the Higgs is localized to the IR brane the effective Yukawa coupling for a SM fermion species f is

$$\lambda_f = \lambda_0 \xi_L(\pi) \xi_R(\pi), \quad (13)$$

where λ_0 is the dimensionless 5d Yukawa coupling. For fermions with one or both components with $\nu < -1/2$ this will be exponentially suppressed. Choosing different $\mathcal{O}(1)$ values for the ν_Ψ allows the entire fermion mass hierarchy to be generated[3].

References

- [1] L. Randall and R. Sundrum, Phys. Rev. Lett. **83**, 3370 (1999) [arXiv:hep-ph/9905221].
L. Randall and R. Sundrum, Phys. Rev. Lett. **83**, 4690 (1999) [arXiv:hep-th/9906064].
- [2] H. Davoudiasl, J. L. Hewett and T. G. Rizzo, Phys. Rev. D **63**, 075004 (2001) [arXiv:hep-ph/0006041]. A. Pomarol, Phys. Lett. B **486**, 153 (2000) [arXiv:hep-ph/9911294].
- [3] Y. Grossman and M. Neubert, Phys. Lett. B **474**, 361 (2000) [arXiv:hep-ph/9912408].
T. Gherghetta and A. Pomarol, Nucl. Phys. B **586**, 141 (2000) [arXiv:hep-ph/0003129].
- [4] K. Agashe, A. Delgado, M. J. May and R. Sundrum, JHEP **0308**, 050 (2003) [arXiv:hep-ph/0308036].

- [5] L. Randall and M. D. Schwartz, JHEP **0111**, 003 (2001) [arXiv:hep-th/0108114]. L. Randall and M. D. Schwartz, Phys. Rev. Lett. **88**, 081801 (2002) [arXiv:hep-th/0108115]. W. D. Goldberger and I. Z. Rothstein, Phys. Rev. Lett. **89**, 131601 (2002) [arXiv:hep-th/0204160]. W. D. Goldberger and I. Z. Rothstein, Phys. Rev. D **68**, 125011 (2003) [arXiv:hep-th/0208060]. K. Agashe, A. Delgado and R. Sundrum, Nucl. Phys. B **643**, 172 (2002) [arXiv:hep-ph/0206099]. K. Agashe, R. Contino and R. Sundrum, Phys. Rev. Lett. **95**, 171804 (2005) [arXiv:hep-ph/0502222].
- [6] B. Abbott *et al.* [D0 Collaboration], Phys. Rev. D **58**, 052001 (1998) [arXiv:hep-ex/9801025]. F. Abe *et al.* [CDF Collaboration], Phys. Rev. Lett. **80**, 2767 (1998) [arXiv:hep-ex/9801014].
- [7] “ATLAS: Detector and physics performance technical design report. Volume 1,” CERN-LHCC-99-14.
“ATLAS detector and physics performance. Technical design report. Vol. 2,” CERN-LHCC-99-15
- [8] CMS Technical Design Report V.1., CERN-LHCC-2006-001,
CMS Technical Design Report V.2., CERN-LHCC-2006-021
- [9] A. Pomarol, Phys. Rev. Lett. **85**, 4004 (2000) [arXiv:hep-ph/0005293].
- [10] N. Arkani-Hamed, M. Porrati and L. Randall, JHEP **0108**, 017 (2001) [arXiv:hep-th/0012148].
- [11] V. Barger, T. Han and D. G. E. Walker, arXiv:hep-ph/0612016.
- [12] F. Maltoni and T. Stelzer, JHEP **0302**, 027 (2003) [arXiv:hep-ph/0208156].
- [13] T. Sjostrand, S. Mrenna and P. Skands, JHEP **0605**, 026 (2006) [arXiv:hep-ph/0603175].
- [14] J. M. Butterworth, B. E. Cox and J. R. Forshaw, Phys. Rev. D **65**, 096014 (2002) [arXiv:hep-ph/0201098].
- [15] J. M. Campbell, J. W. Huston and W. J. Stirling, arXiv:hep-ph/0611148.
- [16] V. D. Barger, J. Ohnemus and R. J. N. Phillips, Int. J. Mod. Phys. A **4**, 617 (1989). G. L. Kane, G. A. Ladinsky and C. P. Yuan, Phys. Rev. D **45**, 124 (1992). C. R. Schmidt and M. E. Peskin, Phys. Rev. Lett. **69**, 410 (1992). A. Brandenburg and J. P. Ma, Phys. Lett. B **298**, 211 (1993). M. Jezabek and J. H. Kuhn, Phys. Lett. B **329**, 317 (1994) [arXiv:hep-ph/9403366]. G. Mahlon and S. J. Parke, Phys. Rev. D **53**, 4886 (1996) [arXiv:hep-ph/9512264].
- [17] A. A. Affolder *et al.* [CDF Collaboration], Phys. Rev. Lett. **84**, 216 (2000) [arXiv:hep-ex/9909042]. B. Abbott *et al.* [D0 Collaboration], Phys. Rev. Lett. **85**, 256 (2000) [arXiv:hep-ex/0002058]. [CDF II Collaboration], arXiv:hep-ex/0612011.
- [18] F. Hubaut, E. Monnier, P. Pralavorio, K. Smolek and V. Simak, Eur. Phys. J. C **44S2**, 13 (2005) [arXiv:hep-ex/0508061].
- [19] T. M. P. Tait, arXiv:hep-ph/9907462.

- [20] [CDF II Collaboration], arXiv:hep-ex/0612011. [D0 Collaboration], arXiv:hep-ex/0609045.
- [21] K. Agashe, A. Belyaev, T. Krupovnickas, G. Perez and J. Virzi, arXiv:hep-ph/0612015.